Materials Research. 2018; 21(2): e20170815
DOI: http://dx.doi.org/10.1590/1980-5373-MR-2017-0815

Multi-Objective Curing Cycle Optimization for Glass Fabric/Epoxy Composites Using Poisson Regression and Genetic Algorithm

Georgios Seretis[a]*, Georgios Kouzilos[a], Dimitrios Manolakos[a], Christopher Provatidis[a]

[a]*School of Mechanical Engineering, National Technical University of Athens, 9 Heroon Polytechniou Str., 15780 Zografou, Athens, Greece*

Received: September 07, 2017; Revised: November 10, 2017; Accepted: December 14, 2017

In this study, a multi-parameter design of experiments, using Taguchi method, has been conducted in order to investigate the optimum curing conditions for glass fabric/epoxy laminated composites, followed by a statistical analysis and genetic algorithm optimization. Heating rate a, temperature T_1 and duration h_1 were treated as independent variables in a L_{25} Taguchi orthogonal array addressing five levels each. Tensile load and flexural strength were examined as pre-selected quality objectives. The results of the analysis of variance performed showed that the significant parameters for both tensile and flexural strength were temperature and duration, at a 95% confidence level. The estimation of the curing parameters for optimum tensile and flexural performance was achieved with an error considerably lower than 1%. The Poisson regression analysis was introduced to achieve a highly accurate regression model, with R^2 greater than 97% for both optimization criteria. Finally, these two regression models were converted into a two-fold function for maximizing both criteria, and used as fitness function for a multi-objective optimization genetic algorithm.

Keywords: *Polymer-matrix composites, Laminates, Cure behavior, Mechanical properties, Poisson regression, Soft-computing.*

1. Introduction

One of the most important processes for epoxy composites production is curing, since most of the final properties of the composites are controlled and affected by the curing cycle applied[1,2]. Many different parameters that affect the curing cycle and its results, such as the relation between the curing temperature (T_{cure}) and the glass transition temperature (T_g)[3], have been widely investigated[3-6]. Alternative curing processes, such as curing using microwaves, have been studied as well[7-10].

Taguchi analysis has been used in many cases to predict the response of composite materials, evaluate the significance of affecting parameters and calculate the optimum conditions/parameters for various types of composite materials and related processes. A.Q. Barbosa et al. used a Taguchi design of experiments to understand the influence of each parameter under study (amount, size and presence of surface treatment) and the interaction between them[11]. The finite element (FE) simulation, the Taguchi technique, and the analysis of variance (ANOVA) techniques were carried out by Thipprakmas to investigate the degree of importance of V-ring indenter parameters[12]. A. K. Parida et al. applied response surface methodology (RSM) to determine the optimum machining conditions leading to minimum surface roughness in drilling of GFRP composite[13]. The experimental plan and analysis is based on the Taguchi L_{27} orthogonal array taking spindle speed (N), feed (f) and diameter of drill bit (d) as important parameters. Rout and Satapathy describe a Taguchi design methodology to determine optimal parameter settings in the development of multiphase hybrid composites consisting of epoxy reinforced with glass-fiber and filled with rice husk particulates[14]. R.A. Kishore et al. performed a Taguchi analysis of the residual tensile strength after drilling in glass fiber reinforced epoxy composites[15]. V.N. Gaitonde et al. investigated and analyzed the parametric influence on delamination in high-speed drilling of carbon fiber reinforced plastic composites[16]. Tsao and Hocheng investigated the delamination associated with various drill bits in drilling of composite materials using Taguchi analysis[17]. Davim and Reis investigated the drilling process on carbon fiber reinforced plastics manufactured by autoclave, performing an experimental study followed by a statistical analysis of the results[18].

Several different methods have been used to analyze the influence of the curing parameters on the final properties of the produced composites. Full factorial approaches are the most commonly used although they employ limited number of levels for each factor, due to the considerably large number of experiments[19,20]. Some studies control only one factor per time, i.e. per experimental series[21]. The central composite rotatable design combined with a quadratic response surface model has been also used[22]. Finally, Taguchi design of experiments has been used combined mostly with linear or quadratic regression models[11].

*e-mail: gio.seretis@yahoo.com

The commonly used Multiple Regression Analyses are based on many different regression models[23-28]. Many efforts have been made in order to achieve a highly accurate multiple regression model[25,27-29]. However, the widely used regression models are quite trivial and their accuracy is in many cases quite low[11].

In order to investigate the optimum curing conditions for glass fabric/epoxy laminated composites, a multi-parameter design of experiments, using Taguchi method, has been conducted in this study, followed by statistical analysis and a genetic algorithm multi-objective optimization. In a L_{25} Taguchi orthogonal array, the parameters heating rate a, temperature T_1 and duration h_1 were treated as independent variables addressing five levels each. The quality objectives examined were tensile load and flexural strength. Flexural strength is of the most important and desired properties of fabric reinforced laminated composites[30-32]. However, composite structures often fail under flexural load[32,33]. Therefore, it is crucial to obtain the optimum flexural strength for these materials, since there is a constant need for their flexural performance improvement. Additionally, tensile performance is important to be optimized for all engineering materials. Analysis of variance results shown that the significant parameters for both tensile and flexural strength were temperature T_1 and duration h_1, at a 95% confidence level. The error of the estimation of the curing parameters for optimum tensile and flexural performance was considerably lower than 1%. However, the widely used regression models achieved quite low accuracy. Therefore, the solution came from a regression analysis that is quite common in epidemiology, sociology and psychology, i.e. Poisson regression. Here, the Poisson regression analysis was introduced to achieve a highly accurate regression model, with R^2 greater than 97% for both optimization criteria. This accuracy has never reported using the widely used regression models. Finally, these two regression models were converted into a two-fold function for maximizing both criteria, and used as fitness function for a multi-objective optimization genetic algorithm.

2. Taguchi design of Experiments

In order to study the entire process parameter space with a small number of experiments only, Taguchi's method uses a special design of orthogonal arrays[34]. The Taguchi approach is a more effective method than traditional design of experiment methods such as factorial design, which is resource and time consuming. With this method the number of experiments to evaluate the influence of control parameters on certain quality properties or characteristics is markedly reduced compared to a full factorial approach. For example, a process with 8 variables, each with 3 states, would require $3^8 = 6561$ experiments to test all variables (full factorial design). However, using Taguchi's orthogonal arrays, only 18 experiments are necessary, i.e. less than 0.3% of the original number of experiments. Taguchi recommends the use of the loss function to determine the deviation between the experimental value of the performance characteristic and the desired value. The loss function is further transformed into an S/N ratio, which is used to rank the influencing parameters according to their impact on the measured value. After that, the significant parameters can be separated from the parameters which are negligible using ANOVA. This allows a prediction of the optimal manufacturing or process parameters[35]. To verify the predicted optimal testing parameters, a confirmation experiment with these parameters should be employed[36,37].

In the calculation of the loss function there are three ways of transformation depending on the desired characteristic of the measured value. The characteristic of the desired value can either be the-lower-the-better, the-higher-the-better or the-nominal-the better. The loss function of the "the-nominal-the-better" quality characteristic (y_k) with m as the mean of the target quality parameter is calculated as shown in Eq. (1) where L_{ij} is the loss function of the ith performance characteristic in the jth experiment.

The loss function of the "the-lower-the-better" and the "the higher- the-better" from the target value of the quality performance characteristic are shown in Eqs. (2) and (3), respectively.

$$L_{ij} = \frac{1}{n}\sum_{k=1}^{n}(y_{ij} - m)^2 \quad (1)$$

$$L_{ij} = \frac{1}{n}\sum_{k=1}^{n} y_{ij}^2 \quad (2)$$

$$L_{ij} = \frac{1}{n}\sum_{k=1}^{n} \frac{1}{y_{ij}^2} \quad (3)$$

In the Taguchi method, the S/N ratio is used to determine the deviation of the performance characteristic from the desired value. The S/N ratio n_{ij} for the ith performance characteristic in the jth experiment can be calculated using the following equation:

$$n_{ij} = -10\log(L_{ij}) \quad (4)$$

Regardless of the category of the performance characteristic, a larger S/N ratio corresponds to a better-quality performance. Therefore, the optimal level of the process parameters is the level with the highest S/N ratio[38,39].

The selection of control factors is the most important part in the design of experiment. Therefore, many factors are initially included so that the non-significant variables can be identified easily. Factors like heating rate (a), temperature (T_1), time (h_1) largely influence the mechanical behavior of the epoxy matrix[19-22] and, consequently, of the laminated composite. The impact of these three factors on tensile

and fracture stresses in glass fabric/epoxy composites is, therefore, studied in this work using an L_{25} orthogonal array design. The selected levels of the three control factors are listed in Table 1. Since to different targets are included in this study, i.e. tensile and flexural performance, the levels of the temperature factor (T_1) should be both below and above T_g temperature, in order to investigate all the curing mechanisms can be achieved[3-5,19-21]. The levels of the time factor (h_1) and the heating rate factor (a) were selected to be in accordance with both the literature[19-21,40] and manufacturers' guides for similar epoxy systems.

3. Experimental Procedure

3.1 Materials

The low-viscosity Araldite GY 783 epoxy resin combined with the low-viscosity, phenol free, modified cycloaliphatic polyamine hardener was used as matrix material for the composite specimens of the present study. The glass transition temperature (*Tg*) was 100°C and the gel time for the specific matrix composition at 20°C and 65% relative humidity (RH), conditioning requirements which were obeyed during the preparation of the composites laminates, was 35 min. Woven E-glass fabric of 282 g/m^2 density was used for matrix reinforcement, as presented in Fig.1. Fig.2 presents an explosive view of the fabrication process together with the E-glass fabric (P) orientations in the composite laminates. The characteristics of the fabric used can be found in Table 2. Since the warp direction is the enhanced one, see Table 2, it is clear that this is the main weave direction. Therefore, the laminae orientations in the stacking sequence of the composites will be based on the warp direction.

3.2 Preparation of E-glass fabric/epoxy composites

Weighed amount of hardener was added into the epoxy resin (monomer) at the manufacturer recommended monomer/hardener proportion, which was a 100:50 by weight ratio, and stirred gently using a laboratory mixer for mechanical stirring for a process time of 5 min at 200 rpm. Subsequently, the matrix mixture was coated and hand-rolled on E-glass fabrics in layer sequence under constant stirring. For each hand lay-up procedure, four layers of E-glass fabric were employed in $[0^o/45^o/-45^o/0^o]_T$ sequence. Before the first layer coating, the surface on which the specimens were produced was covered by release paste wax. The hand lay-up procedure applied, along with the stacking sequence of the specimens, is presented in Fig.2 through a 3D model in explosive view mode. The processing temperature for the hand lay-up process applied was 23±1°C (ambient temperature). To achieve a 40±1% by volume epoxy proportion in all specimens, both the fabric and the matrix mixture used for

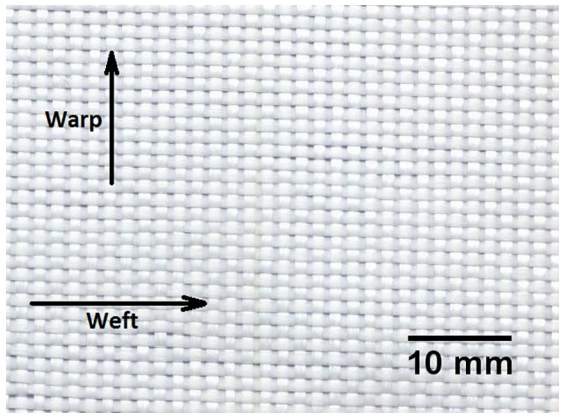

Figure 1. The woven E-glass fabric used in layer orientation 0º.

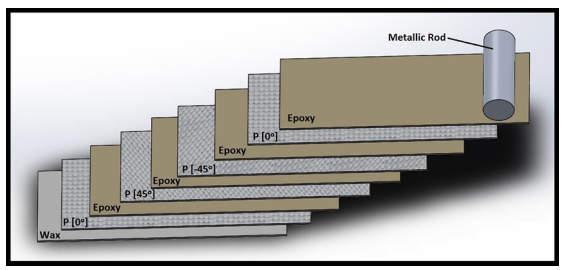

Figure 2. Layer sequence and fabric orientation on the tested $[0^o/45^o/-45^o/0^o]_T$ laminates.

Table 1. Parameters and Design of Experiments (DOE) Levels.

Control factor	Level					Units
	I	II	III	IV	V	
Heating Rate ***a***	1	2	3	4	5	ºC/min
Temperature $\boldsymbol{T_1}$	50	80	100	120	140	ºC
Time $\boldsymbol{h_1}$	2	4	6	8	10	h

Table 2. Characteristics of the glass fabrics used.

	Warp	Weft
Fiber description	Glass EC11 204 fiber	Glass EC11 204 fiber
Thread count (ends/cm)	8	6
Weight distribution (%)	57	43

coating were weighed before each hand lay-up process and after solidification.

The dimensions of each specimen which underwent 3-point bending tests were 93.6 × 12.7 ×1.1 mm, as in accordance with ASTM D790-03 test method. The specimens which underwent tensile test had a total size of 102 × 6 × 1.1 mm according to ASTM D3039/3039M. All specimens were cut at their testing dimensions using a Struers Discotom-2 along with a 40A25 cut-off wheel. To evaluate if tabs were needed on the holding regions of the specimens, the theoretical tab limits were marked on the specimens, as indicated from the aforementioned ASTM standard method. Thus, if the failure occurs between the two theoretical tab limits (theoretical control region) no tabs are needed. As it can be seen in Fig.3, the failure occurred into the theoretical control region and, therefore, no tabs are recommended by the ASTM standard used.

For each experiment number (run number) of the Taguchi design of experiments, see Tables 3 and 4, five specimens were prepared and underwent each test (five specimens for each tensile and five for each flexural test).

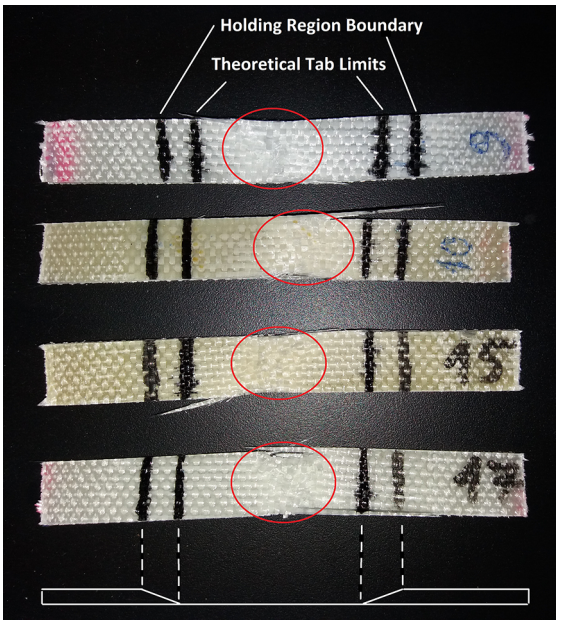

Figure 3. Holding region boundaries and theoretical tab limits for the composite laminates which underwent tensile tests.

Table 3. Taguchi L_{25} OA response values and S/N ratio for Load in Tensile tests.

Run No	Heating Rate *a*	Temperature T_1	Time h_1	Load (N)	S/N Ratio (dB)
1	I	I	I	2612,00	68,3395
2	I	II	II	3690,00	71,3405
3	I	III	III	2797,50	68,9354
4	I	IV	IV	3397,00	70,6219
5	I	V	V	2971,00	69,4581
6	II	I	II	2736,75	68,7447
7	II	II	III	3059,00	69,7116
8	II	III	IV	3643,00	71,2292
9	II	IV	V	3275,00	70,3042
10	II	V	I	3122,00	69,8887
11	III	I	III	2894,00	69,2300
12	III	II	IV	3178,50	70,0444
13	III	III	V	2831,00	68,7542
14	III	IV	I	3307,50	70,3900
15	III	V	II	3309,00	70,3939
16	IV	I	IV	2938,00	69,3610
17	IV	II	V	2769,00	68,8465
18	IV	III	I	3156,00	69,9827
19	IV	IV	II	3862,33	71,7370
20	IV	V	III	3629,50	71,1969
21	V	I	V	2526,00	68,0487
22	V	II	I	2594,50	68,2811
23	V	III	II	3409,50	70,6538
24	V	IV	III	3277,50	70,3109
25	V	V	IV	3542,50	70,9862

Table 4. Taguchi L_{25} OA response values a nd S/N ratio for Stress in Flexural tests.

Run No	Heating Rate *a*	Temperature T_1	Time h_1	Stress (MPa)	S/N Ratio (dB)
1	I	I	I	143,333	42,7872
2	I	II	II	327,333	50,2998
3	I	III	III	286,333	49,1374
4	I	IV	IV	442,667	52,9215
5	I	V	V	299,5	49,7259
6	II	I	II	295	49,3964
7	II	II	III	346	50,7815
8	II	III	IV	369	51,3405
9	II	IV	V	420	52,465
10	II	V	I	371	51,3875
11	III	I	III	307	49,7428
12	III	II	IV	362,5	51,1862
13	III	III	V	318,5	49,9065
14	III	IV	I	349	50,8565
15	III	V	II	297	49,4551
16	IV	I	IV	277,5	48,8653
17	IV	II	V	335,5	50,5139
18	IV	III	I	235	47,4214
19	IV	IV	II	402,667	52,0989
20	IV	V	III	387,5	51,7654
21	V	I	V	306,5	45,8673
22	V	II	I	149,5	43,4928
23	V	III	II	357,5	51,0655
24	V	IV	III	377,5	51,5383
25	V	V	IV	477,5	53,5795

3.3 Curing of E-glass fabric/epoxy composites

All specimens left in ambient temperature for 6 hours before the curing conditions of the Taguchi design of experiments, as described in Tables 3 and 4, were applied. Therefore, the complete curing cycle applied is presented in Fig.4, where parameter a, T_1 and h_1 represent the heating rate [°C/min], the temperature of the first curing step [°C] and the duration of the first curing step [h], respectively. The selected values for each parameter under study (i.e. the design of experiment levels) can be found in Table 1.

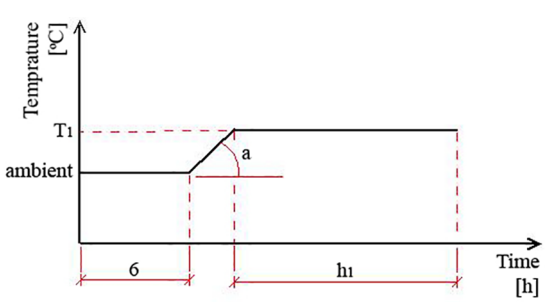

Figure 4. The curing cycle applied together with the parameters of the Taguchi design of the experiments. Ambient temperature is considered equal to 23±1°C, a is the heating rate [°C/min], T_1 is the curing temperature [°C] and h_1 is the curing time [h].

The curing temperature (T_{cure}) can be either higher or lower of the glass transition temperature (T_g)[3-5]. When $T_{cure} > T_g$, the reaction proceeds rapidly at a rate driven by chemical kinetics. When $T_{cure} = T_g$, vitrification takes place (i.e. material solidifies). Finally, when $T_{cure} < T_g$, the reaction rate decelerates and becomes diffusion-controlled. In order to include all the aforementioned mechanisms in the Taguchi design of experiments, apart from the T_g temperature, two different temperatures under T_g were selected as well as two different temperatures over it, see Table 1.

3.4 Experimental set-up and tests

The test machine used for the both tensile and 3-point bending tests was an Instron 4482 of 100 kN capacity. In accordance with the ASTM standard methods used, i.e. D790-03 and D3039/3039M, all tests were performed in a standard laboratory atmosphere (23±1ºC and 50±5% relative humidity). Test conditioning was kept constant for 6 hours before each test. To meet the test method's span-to-depth specification, the support span was set at 52 mm for the flexural tests. The recommended from the ASTM methods test speed of 2 mm/min was applied on both tensile and 3-point bending tests.

4. Results and Discussion

4.1 Taguchi results

In terms of the S/N ratio for stresses and load value, the higher the better. This can be calculated as logarithmic transformation of loss function (Eq. 2). The calculated signal to noise (S/N) ratio for each experiment is presented in Tables 3 and 4 for tensile and flexural test respectively, along with their experimental results. S/N ratio is an important characteristic in order to achieve robustness in Taguchi design of experiment, desired output is known as the signal and variability caused by factors is known as noise.

The main effects plot for the main effect terms in tensile load for factors a, T_1, and h_1 are shown in Fig.5. From the main effect plots, it has been observed that the tensile load of the composite increases for heating rate values ranging from 1ºC/min to 2ºC/min and from 3ºC/min to 4 ºC/min and decreases with faster heating. The curing temperature affects the tensile load increase of the composite material as well. Specifically, while temperature is ranging from 50 ºC to 80 ºC an increase in load occurred. Subsequently, from 80 ºC to 100 ºC the load remains constant and from 100 ºC up to 120 ºC it increases. Further increase in temperature leads to an opposite outcome, showing downgrading of mechanical properties due to thermal decomposition of long chains of the epoxy matrix. With increased temperature, free radicals and developing polymer chains become more fluid as a consequence of decreased viscosity and they react to a greater extent. This results in a more complete polymerization reaction and consequently greater cross-linking[41]. The increase in the degree of polymerization of composites may lead to improved mechanical properties and increased wear resistance[42]. Therefore, it is expected that by increasing the process temperature the performance of the produced composite may be consequently increased as well. It is known that while the temperature increases, the thermal expansion coefficient of epoxy/fiberglass composites is being increased as well[43]. However, it increases with a different rate of change for low and for high temperature values. Specifically, for low temperature values the rate of change is quite low and while increasing the temperature this rate takes considerably greater values. Due to the high values of thermal expansion coefficient for temperatures greater than 120 ºC, voids may be formed on the epoxy/fiberglass interfaces, leading in this manner to a consequent performance drop[44]. The curing time increase affects the increase of the tensile load of the composite material while factor h_1 is ranging from 2 to 4 hours. From 4 to 6 hours the tensile load decreases. From 6 to 8 hours the load increases and for greater values of h_1 the load decreases. From the main effect plots of Fig.6, it can be observed that the flexural strength of the composite responses similarly with the tensile load while changing the heating rate value. The temperature increase affects the flexural strength of the composite in the same manner as it affects the tensile load, as well. The h_1 factor, which represents the curing duration, has a positive effect in terms of increasing the flexural strength of the composite. For h_1 values up to 8 hours a rise of load can be observed and with further increase of h_1 factor the flexural strength decreases. In general, an initial performance increase can be observed for both tensile and flexural tests while the curing time increases. Subsequently, the performance shows a decreasing trend. For short curing times, it is known that a curing time increase leads to a subsequent strength increase[45]. The curing cycle had a significant effect on both the tensile and flexural performance of the composites. It is known that the curing cycle affects the polymer chains of the matrix[46-49] as well as the quality of the fibril/epoxy interface[44]. Due to the different thermal expansion coefficient of the involved components, i.e. fibrils and epoxy matrix, while a composite laminate undergoes thermal cycles during curing, voids may be formed on the fibril/epoxy interfaces leading to an interface interruption[44].

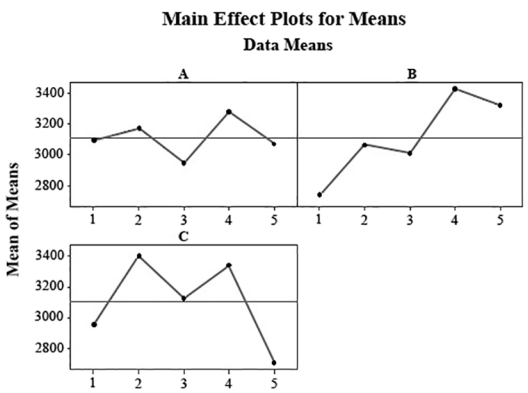

Figure 5. Main effect plots for tensile load for a (heating rate), T_1 (temperature) and h_1 (time) factors.

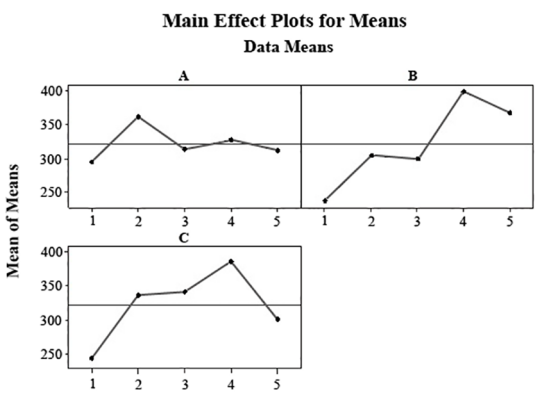

Figure 6. Main effect plots for flexural strength for a (heating rate), T_1 (temperature) and h_1 (time) factors.

4.2 Analysis of Variance

Analysis of variance (ANOVA) is a statistical tool which examines the hypothesis that the means of two or more populations are equal. It evaluates the significance of one or more factors by comparing the response variable means at the different factor levels. It was observed that the significant factor for tensile and flexural strength was temperature and time at 95% confidence level, see Tables 5 and 6. In order to evaluate the analysis, conformation tests were performed (Tables 7 and 8) by comparing actual values and optimal ones. The optimal values can be predicted using Eq. (5)[50].

$$n_{opt} = n_m + \sum_{i=1}^{q} (n_i - n_m) \quad (5)$$

where: η_m is the total mean of the response under consideration (tensile load and flexural strength, respectively); η_i is the mean response value at the optimum level and q is the number of the curing process control factors that significantly affect the response of the composites after curing.

4.3 Poisson Regression Analysis with Backward Elimination

Regression analysis is a statistical process for approximating the relationships between variables. It is a method for modelling different variables. It helps to understand how the dependent variable deviates when any one of the independent variables is changed[51]. Poisson regression is a regression method, which employees a logarithmic transformation that compensates for skewness, prevents a negative predicted value, and also includes the proportionality between variance and the mean[52].

Therefore, if Y has a Poisson distribution, then a log-linear model can be constructed as

$$ln\,\hat{Y} = \alpha + \beta_1 X_1 + \beta_2 X_2 + \cdots + \beta_k X_k \quad (6)$$

The difficulty of the above form is that the prediction is in terms of log counts. However, in practice actual counts are needed. To handle this difficulty, both sides have to be exponiated.

$$e^{\ln \hat{Y}} = e^{(\alpha + \beta_1 X_1 + \beta_2 X_2 + \cdots + \beta_k X_k)} \quad (7)$$

or equally

$$\hat{Y} = e^{(\alpha + \beta_1 X_1 + \beta_2 X_2 + \cdots + \beta_k X_k)} \quad (8)$$

In this form, the predicted value of Y is in counts.

The backward elimination applied to all the variants included in the regression. The effect of removing a variable on residual mean square (MS_{res}) was assessed for each variable, and the variable with the least effect on increasing MS_{res} was removed if it did not increase the F ratio for removal, *Fout*. *Fout* was set at 4. The process continued until removal caused a significant change in MS_{res}, when that variant was left in and no further removals were done.

Poisson regression analysis, together with backward elimination, was carried out for tensile load and flexural strength taking all factors (a, T_1, h_1) as independent variables. In the case of flexural strength regression model, only the significant factors (T_1, h_1) were kept, since the heating rate factor (a) was eliminated by the backward elimination process. Normal probability of regression equation was also plotted in Figs.7 and 8 for tensile load and flexural strength respectively. The regression coefficients of tensile load and flexural stress values are provided in Tables 9 and 10 respectively.

$$Tensile\ Load = e^{Y_1'} \quad (9)$$

where

$Y_1' = -0.3 - 8.8 \times a + 0.524 \times T_1 - 0.83 \times h_1 + 0.784 \times a^2 - 0.002901 \times T_1^2 + 1.547 \times h^2 + 5.31 \times a \times h_1 - 0.1979 \times T_1 \times h_1 + 0.000003 \times T_1^3 - 0.285 \times h_1^3 - 0.3327 \times a \times h^2 + 0.00099 \times T_1^2 \times h_1 + 0.01975 \times T_1 \times h^2 + 0.0153 \times h_1^4 + 0.03159 \times a^2 \times h^2 + 0.126 \times a \times h_1^3 - 0.000001 \times T_1^3 \times h_1 - 0.000064 \times T_1^2 \times h^2 - 0.000481 \times T^1 \times h^3 - 0.00573 \times a \times h^4$

$$Flexural\ Strength = e^{Y_2'} \quad (10)$$

where

$Y_2' = 4.6336 + 0.009461 \times T_1 + 0.1188 \times h^1 - 0.000792 \times T_1 \times h_1$

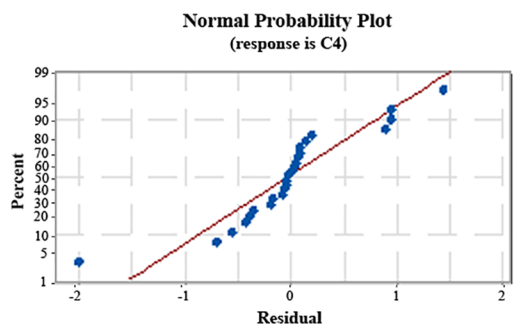

Figure 7. Normal probability of regression equation for tensile load.

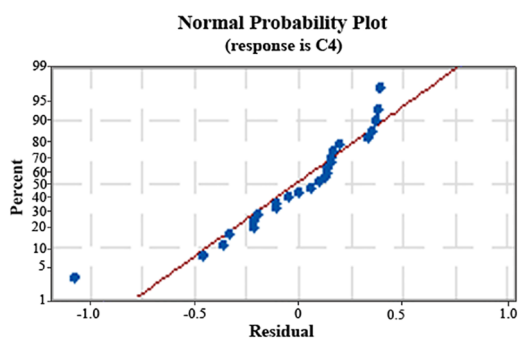

Figure 8. Normal probability of regression equation for flexural strength.

Table 5. ANOVA for Tensile load value, without interaction, $F_{0,05,4,12=3,26,}$.

Source	dF	Sum of squares	Mean square	F-value	P value	C (%)
a	4	293004	73251	0,80	0,367	6,62
T_1	4	1447822	361955	3,96*	0,003*	32,71
h_1	4	1588652	397163	4,34*	0,010*	35,89
Error	12	1097301	91442			
Total	24	4426778				

*Significant at 95% confidence level.

Table 6. ANOVA for Flexural stress value, without interaction, $F_{0,05,4,12=3,26,}$.

Source	dF	Sum of squares	Mean square	F-value	P value	C (%)
a	4	12361	3090	1,18	0,367	6,92
T_1	4	78612	19653	7,53*	0,003*	44,02
h_1	4	56284	14071	5,39*	0,010*	31,52
Error	12	31335	2611			
Total	24	178591				

*Significant at 95% confidence level.

Table 7. Confirmation table for tensile load.

Parameter	Optimal Parameter	
	a = 4 ºC/min, T_1 = 120 ºC, h_1 = 4 h	
	Experimental	Predicted
Load (N)	3862,33	3878,10
Error %	0,41 %	

Table 8. Confirmation table for flexural strenth.

Parameter	Optimal Parameter	
	a = 2 ºC/min, T_1 = 120 ºC, h_1 = 8 h	
	Experimental	Predicted
Flexural Stress (N)	498,70	501,93
Error %	0,65%	

Taking this data into consideration it is possible to formulate an equation that allows for the prediction of the mechanical behavior of the composite by altering the temperature and the curing time. Figs. 9 and 10 present a comparison between the theoretical model, see Eqs. (9) and (10), and the experimental results for both tensile and flexural tests. It can be easily observed that the experimental and theoretical results always show a perfect correlation. Therefore, the equations of the theoretical model above are a useful tool to accurately predict both the tensile (R^2=97.05%) and flexural (R^2=98.11%) response of the cured composites.

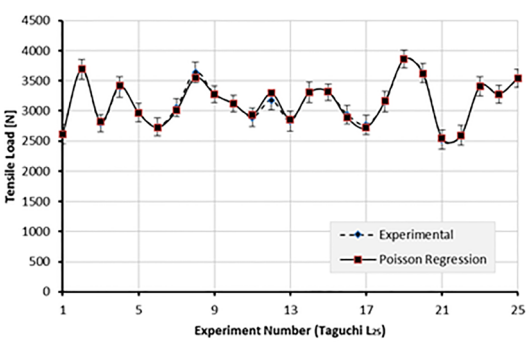

Figure 9. Comparison between the experimental results and the theoretical values of tensile load.

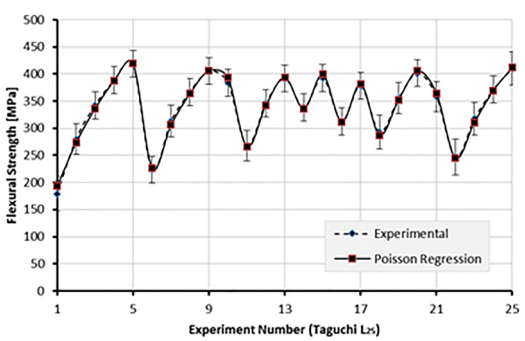

Figure 10. Comparison between the experimental results and the theoretical values of flexural strength.

4.4 Process optimization using a genetic algorithm

The aim of the optimization procedure is to determine the optimal values of the curing parameters (a, T_1, h_1) that contribute to the maximum values for both criteria; *Tensile Load* and *Flexural Strength*. The solution of the aforementioned task lies on the multi-objective optimization concept. The Poisson regression models for both criteria, i.e. Eqs.(9) and (10), were converted into a MATLAB® function for maximizing *Tensile Load* and *Flexural Strength*. Therefore, the two-fold function of eq. (11) was created.

Table 9. Regression coefficients of tensile model with all factors.

Term	Coef	SE Coef	95% CI		Z-Value	P-Value
Constant	-0.30	1.33	(-2.90;	2.31)	-0.22	0.824
a	-8.80	2.15	(-13.02;	-4.58)	-4.09	0.000
T_1	0.524	0.131	(0.268;	0.781)	4.01	0.000
h_1	-0.83	1.12	(-3.03;	1.37)	-0.74	0.461
a^2	0.784	0.167	(0.457;	1.111)	4.70	0.000
T_1^2	-0.002901	0.000848	(-0.004563;	-0.001239)	-3.42	0.001
h_1^2	1.547	0.672	(0.230;	2.863)	2.30	0.021
$a*h_1$	5.31	1.45	(2.47;	8.15)	3.67	0.000
T_1*h_1	-0.1979	0.0484	(-0.2928;	-0.1030)	-4.09	0.000
T_1^3	0.000003	0.000002	(-0.000000;	0.000006)	1.94	0.053
h_1^3	-0.285	0.109	(-0.498;	-0.073)	-2.63	0.009
a^2*h_1	-0.3327	0.0728	(-0.4754;	-0.1900)	-4.57	0.000
$a*h_1^2$	-1.177	0.357	(-1.876;	-0.479)	-3.30	0.001
$T_1^2*h_1$	0.000990	0.000248	(0.000504;	0.001477)	3.99	0.000
$T_1*h_1^2$	0.01975	0.00507	(0.00981;	0.02969)	3.89	0.000
h_1^4	0.01530	0.00550	(0.00452;	0.02607)	2.78	0.005
$a*a*h_1^2$	0.03159	0.00741	(0.01707;	0.04612)	4.26	0.000
$a*h_1^3$	0.1260	0.0403	(0.0471;	0.2049)	3.13	0.002
$T_1^3*h_1$	-0.000001	0.000000	(-0.000002;	-0.000000)	-3.43	0.001
$T_1^2*h_1^2$	-0.000064	0.000017	(-0.000097;	-0.000031)	-3.84	0.000
$T_1*h_1^3$	-0.000481	0.000128	(-0.000731;	-0.000231)	-3.77	0.000
$a*h_1^4$	-0.00573	0.00183	(-0.00932;	-0.00214)	-3.13	0.002

Table 10. Regression coefficients of flexural model with significant factors.

Term	Coef	SE Coef	95% CI		Z-Value	P-Value
Constant	4.6336	0.0952	(4.4469;	4.8202)	48.66	0.000
T_1	0.009461	0.000879	(0.007739;	0.011183)	10.77	0.000
h_1	0.1188	0.0135	(0.0924;	0.1453)	8.80	0.000
T_1*h_1	-0.000792	0.000126	(-0.001039;	-0.000545)	-6.28	0.000

$$\max f(a,T_1,h_1)=\begin{cases}\max Tensile\ Load=\min(1/Tensile\ Load)=\min(1/e^{Y_1})\\ \max Flexural\ Strength=\min(1/Flexural\ Strength)=\min(1/e^{Y_2})\end{cases} \quad (11)$$

where

$Y_1' = -0.3 - 8.8 \times a + 0.524 \times T_1 - 0.83 \times h_1 + 0.784 \times a^2 - 0.002901 \times T_1^2 + 1.547 \times h^2 + 5.31 \times a \times h_1 - 0.1979 \times T_1 \times h_1 + 0.000003 \times T_1^3 - 0.285 \times h_1^3 - 0.3327 \times a \times h^2 + 0.00099 \times T_1^2 \times h_1 + 0.01975 \times T_1 \times h^2 + 0.0153 \times h_1^4 + 0.03159 \times a^2 \times h^2 + 0.126 \times a \times h_1^3 - 0.000001 \times T_1^3 \times h_1 - 0.000064 \times T_1^2 \times h^2 - 0.000481 \times T^1 \times h^3 - 0.00573 \times a \times h^4$

and

$Y_2' = 4.6336 + 0.009461 \times T_1 + 0.1188 \times h^1 - 0.000792 \times T_1 \times h_1$

Eq. (11) was the fitness function for the multi-objective optimization GA of MATLAB® optimization toolbox. For the optimization process a population size of 45 individuals (15 * number of variables) was specified to evolve for 500 generations with 0.8 probability single point crossover and a constraint dependent mutation function. The algorithmic parameter values were selected as recommended by the optimization toolbox employed, i.e. the migration interval was set to 20; migration fraction was set to 0.2 and Pareto fraction was set to 0.35.

The Pareto-optimal solutions obtained together with their corresponding performance values are summarized in Table 11. The average distance between individuals (candidate solutions) referring to the objective values is depicted in Fig.11. As can be seen in Table 11, the minimum individual distance was obtained for solutions 1 and 2. Therefore, the respective Pareto-optimal fonts indicate that the curing process is optimum, as per the maximization of both tensile and flexural performance, for a = 1 (ºC/min), T_1 = 85 (ºC) and h_1 = 10 (h).

Table 11. Pareto font-function values and optimal curing parameters.

Solution no.	a (ºC/min)	T_1 (ºC)	h_1 (h)	Pareto distance
1	1.001841317	139.9999999	9.999999959	1.6914
2	1.000105286	85.51085564	9.997251776	1.4935
3	1.001847642	139.4348674	9.99881099	1.6890
4	1.001838635	135.9951147	9.999994125	1.6747
5	1.000105286	85.51085564	9.997251776	1.4935
6	1.001731003	137.6706621	9.999573415	1.6816
7	1.00182876	135.1332839	9.999991494	1.6711
8	1.001841317	139.9999999	9.999999959	1.6914
9	1.008023956	136.3610771	9.990931862	1.6788
10	1.014562832	126.9283418	9.986363612	1.6438
11	1.001839871	138.3768794	9.999494526	1.6846
12	1.079739416	118.477614	9.971796304	1.6464
13	1.001841216	137.2358606	9.999992492	1.6798
14	1.00264489	133.0118608	9.979005419	1.6616
15	1.001839235	139.0998201	9.999996542	1.6876
16	1.008728622	134.1460715	9.999806411	1.6706

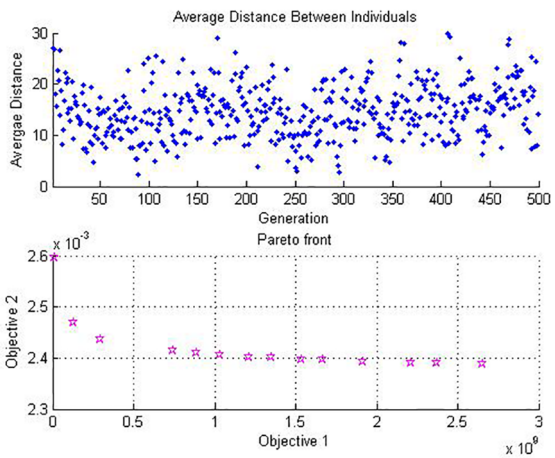

Figure 11. Average distance between individuals per generation and Pareto front.

5. Conclusions

Woven E-glass fabric/epoxy laminated composites were produced and underwent tensile and flexural testing according to a L_{25} Taguchi design of experiments. Based on the experimental results as well as the subsequent statistical analysis and genetic algorithm the following remarks may be drawn:

(a) The significant parameters for both tensile and flexural strength are temperature (T_1) and duration (h_1), at a 95% confidence level. Therefore, for slow temperature increase values, i.e. 1-5 °C/min, the effect of the heating rate a on the performance of the cured laminated composite is not considerable.

(b) The estimation of the curing parameters for optimum tensile and flexural performance can be achieved with an error considerably lower than 1%. More specifically, the error of the calculated optimum tensile performance was 0.41% and of the flexural performance 0.65%.

(c) The optimum performance was obtained for temperature T_1 values greater than the glass transition temperature T_g. It is known that when $T_{cure} > T_g$, the reaction proceeds rapidly at a rate driven by chemical kinetics and when $T_{cure} < T_g$, the reaction rate decelerates and becomes diffusion-controlled. Therefore, it is obvious that both tensile and flexural performance of the epoxy matrix laminated composites is mainly controlled by the chemical kinetics.

(d) Poisson Regression Analysis, together with backward elimination, led to a theoretical model, the correlation of which with the experimental results was almost perfect. Therefore, the Poisson regression theoretical model can accurately predict both the tensile and flexural response of the cured composites.

(e) The optimum curing process, as regards the maximization of both tensile and flexural performance, can be obtained for temperature T_1 lower than the glass transition temperature T_g (diffusion-controlled reaction). Additionally, even if the heating rate a is not a significant factor, the optimum curing process requires a low a value, equal to 1 ºC/min.

6. References

1. Gao L, Zhang Q, Guo J, Li H, Wu J, Yang X, et al. Effects of the amine/epoxy stoichiometry on the curing behavior and glass transition temperature of MWCNTs-NH2/epoxy nanocomposites. *Thermochimica Acta*. 2016;639:98-107.

2. Fu Y, Zhong, WH. Cure kinetics behavior of a functionalized graphitic nanofiber modified epoxy resin. *Thermochimica Acta*. 2011;516(1-2):58-63.

3. Moussa O, Vassilopoulos AP, Keller T. Effects of low-temperature curing on physical behavior of cold-curing epoxy adhesives in bridge construction. *International Journal of Adhesion and Adhesives*. 2012;32:15-22.

4. Ellis B. *Chemistry and Technology of Epoxy Resins*. Dordrecht: Springer; 1993.

5. Wisanrakkit G, Gillham JK. Glass transition temperature (Tg) as an index of chemical conversion for high-Tg amine/epoxy system: Chemical and diffusion controlled reaction kinetics. *Journal of Applied Polymer Science*. 1990;41(11-12):2885-2929.

6. Maljaee H, Ghiassi B, Lourenço PB. Effect of synergistic environmental conditions on thermal properties of a cold curing epoxy resin. *Composites Part B: Engineering*. 2017;113:152-163.

7. Kwak M, Robinson P, Bismarck A, Wise R. Microwave curing of carbon-epoxy composites: Penetration depth and material characterisation. *Composites Part A: Applied Science and Manufacturing*. 2015;75:18-27.

8. Johnston K, Pavuluri SK, Leonard MT, Desmulliez MPY, Arrighi V. Microwave and thermal curing of an epoxy resin for microelectronic applications. *Thermochimica Acta*. 2015;616:100-109.

9. De Vergara UL, Sarrionandia M, Gondra K, Aurrekoetxea J. Polymerization and curing kinetics of furan resins under conventional and microwave heating. *Thermochimica Acta*. 2014;581:92-99.

10. Mijovic J, Fishbain A, Wijaya J. Mechanistic modeling of epoxy amine kinetics. 2. Comparison of kinetics in thermal and microwave fields. *Macromolecules*. 1992;25(2):986-989.

11. Barbosa AQ, da Silva LFM, Abenojar J, Figueiredo M, Öchsner A. Toughness of a brittle epoxy resin reinforced with micro cork particles: Effect of size, amount and surface treatment. *Composites Part B: Engineering*. 2017;114:299-310.

12. Thipprakmas S. Application of Taguchi technique to investigation of geometry and position of V-ring indenter in fine-blanking process. *Materials and Design (1980-2015)*. 2010;31(5):2496-2500.

13. Parida AK, Routara BC, Bhuyan RK. Surface roughness model and parametric optimization in machining of GFRP composite: Taguchi and Response surface methodology approach. *MaterialsToday: Proceedings*. 2015;2(4-5):3065-3074.

14. Rout AK, Satapathy A. Study on mechanical and tribo-performance of rice-husk filled glass-epoxy hybrid composites. *Materials and Design*. 2012;41:131-141.

15. Kishore RA, Tiwari R, Dvivedi A, Singh I. Taguchi analysis of the residual tensile strength after drilling in glass fiber reinforced epoxy composites. *Materials and Design*. 2009;30(6):2186-2190.

16. Gaitonde VN, Karnik SR, Rubio JC, Correia AE, Abrão AM, Davim JP. Analysis of parametric influence on delamination in high-speed drilling of carbon fiber reinforced plastic composites. *Journal of Materials Processing Technology*. 2008;203(1-3):431-438.

17. Tsao CC, Hocheng H. Taguchi analysis of delamination associated with various drill bits in drilling of composite material. *International Journal of Machine Tools and Manufacture*. 2004;44(10):1085-1090.

18. Davim JP, Reis P. Drilling carbon fiber reinforced plastics manufactured by autoclave - experimental and statistical study. *Materials and Design*. 2003;24(5):315-324.

19. Davies LW, Day RJ, Bond D, Nesbitt A, Ellis J, Gardon E. Effect of cure cycle heat transfer rates on the physical and mechanical properties of an epoxy matrix composite. *Composites Science and Technology*. 2007;67(9):1892-1899.

20. Kumar DS, Shukla MJ, Mahato KK, Rathore DK, Prusty RK, Ray BC. Effect of post-curing on thermal and mechanical behavior of GFRP composites. *IOP Conference Series: Materials Science and Engineering*. 2015;75:012012. DOI: 10.1088/1757-899X/75/1/012012

21. Aruniit A, Kers J, Krumme A, Poltimäe T, Tall K. Preliminary Study of the Influence of Post Curing Parameters to the Particle Reinforced Composite's Mechanical and Physical Properties. *Materials Science*. 2012;18(3):256-261.

22. Sultania M, Rai JSP, Srivastava D. Process modeling, optimization and analysis of esterification reaction of cashew nut shell liquid (CNSL)-derived epoxy resin using response surface methodology. *Journal of Hazardous Materials*. 2011;185(2-3):1198-1204.

23. Guo H, Wang X, Gao Z. Uncertain linear regression model and its application. *Journal of Intelligent Manufacturing*. 2017;28(3):559-564. DOI: 10.1007/s10845-014-1022-1024

24. Tangjitsitcharoen S, Thesniyom P, Ratanakuakangwan S. Prediction of surface roughness in ball-end milling process by utilizing dynamic cutting force ratio. *Journal of Intelligent Manufacturing*. 2017;28(1):13-21. DOI: 10.1007/s10845-014-0958-8

25. Luangpaiboon P, Boonhao S, Montemanni R. Steepest ant sense algorithm for parameter optimization of multi-response processes based on taguchi design. *Journal of Intelligent Manufacturing*. 2016. DOI: 10.1007/s10845-016-1257-3

26. Sharma N, Kumar K, Raj T, Kumar V. Porosity exploration of SMA by Taguchi, regression analysis and genetic programming. *Journal of Intelligent Manufacturing* . 2016. DOI: 10.1007/s10845-016-1236-8

27. Li C, Li L, Tang Y, Zhu Y, Li L. A comprehensive approach to parameters optimization of energy-aware CNC milling. *Journal of Intelligent Manufacturing*. 2016. DOI: 10.1007/s10845-016-1233-y

28. Li H, Wang Y, Zhao P, Zhang X, Zhou P. Cutting tool operational reliability prediction based on acoustic emission and logistic regression model. *Journal of Intelligent Manufacturing*. 2015;26(5):923-931. DOI: 10.1007/s10845-014-0941-4

29. Jurkovic Z, Cukor G, Brezocnik M, Brajkovic T. A comparison of machine learning methods for cutting parameters prediction in high speed turning process. *Journal of Intelligent Manufacturing*. 2016. DOI: 10.1007/s10845-016-1206-1

30. Ferdosian F, Zhang Y, Yuan Z, Anderson M, Xu C. Curing kinetics and mechanical properties of bio-based epoxy composites comprising lignin-based epoxy resins. *European Polymer Journal*. 2016;82:153-165.

31. Joosten MW, Agius S, Hilditch T, Wang C. Effect of residual stress on the matrix fatigue cracking of rapidly cured epoxy/anhydride composites. *Composites Part A: Applied Science and Manufacturing*. 2017;101:521-528.

32. Seretis GV, Kouzilos G, Manolakos DE, Provatidis CG. On the graphene nanoplatelets reinforcement of hand lay-up glass fabric/epoxy laminated composites. *Composites Part B: Engineering*. 2017;118:26-32.

33. Omrani E, Barari B, Maghadam AD, Rohatgi PK, Pillai KM. Mechanical and tribological properties of self-lubricating bio-based carbon-fabric epoxy composites made using liquid composite molding. *Tribology International*. 2015;92:222-232.

34. Montgomery DC. *Design and Analysis of Experiments*. New York: John Wiley & Sons; 2001.

35. Rashmi, Renukappa NM, Suresha B, Devarajaiah RM, Shivakumar KN. Dry sliding wear behaviour of organo-modified montmorillonite filled epoxy nanocomposites using Taguchi's techniques. *Materials & Design*. 2011;32(8-9):4528-4536.

36. Naghibi S, Sani MAF, Hosseini HRM. Application of the statistical Taguchi method to optimize TiO_2 nanoparticles synthesis by the hydrothermal assisted sol-gel technique. *Ceramics International*. 2014;40(3):4193-4201.

37. Olivia M, Nikraz H. Properties of fly ash geopolymer concrete designed by Taguchi method. *Materials & Design (1980-2015)*. 2012;36:191-198.

38. Kim KD, Han DN, Kim HT. Optimization of experimental conditions based on the Taguchi robust design for the formation of nano-sized silver particles by chemical reduction method. *Chemical Engineering Journal*. 2004;104(1-3):55-61.

39. Mehat NM, Kamaruddin S. Investigating the Effects of Injection Molding Parameters on the Mechanical Properties of Recycled Plastic Parts Using the Taguchi Method. *Materials and Manufacturing Processes*. 2011;26(2):202-209.

40. Lu S, Chen D, Wang X, Shao J, Ma K, Zhang L, et al. Real-time cure behaviour monitoring of polymer composites using a highly flexible and sensitive CNT buckypaper sensor. *Composites Science and Technology*. 2017;152:181-189.

41. Park SH, Lee CS. The difference in degree of conversion between light-cured and additional heat-cured composites. *Operative Dentistry*. 1996;21(5):213-217.

42. Daronch M, Rueggeberg FA, De Goes MF. Monomer conversion of pre-heated composite. *Journal of Dental Research*. 2005;84(7):663-667.

43. McElroy DL, Weaver FJ, Bridgman C. Thermal expansion of epoxy-fiberglass composite specimens. *International Journal of Thermophysics*. 1988;9(2):233-243.

44. Rudd RM, Ghafarian SR, Taherkhani A. The Effects of Post Curing Process on the Mechanical Properties of Glass Fiber/ Phenol -Formaldehyde Molded Composites. *Journal of Basic and Applied Scientific Research*. 2013;3(1s):36-39.

45. Dolez P, Marek M, Love BJ. Photopolymerizable acrylic resin: effect of curing time and temperature. *Journal of Applied Polymer Science*. 2001;82(3):546-554.

46. Kim H, Char K. Dielectric Changes During the Curing of Epoxy Resin Based on the Diglycidyl Ether of Bisphenol A (DGEBA) with Diamine. *Bulletin of the Korean Chemical Society*. 1999;20(11):1329-1334.

47. Wurster DE, Bhattacharjya S, Flanagan DR. Effect of Curing on Water Diffusivities in Acrylate Free Films as Measured via a Sorption Technique. *AAPS PharmSciTech*. 2007;8(3):E71. DOI: 10.1208/pt0803071

48. Kozakiewicz J, Rokicki G, Przybylski J, Sylwestrzak K, Parzuchowski PG, Tomczyk KM. Studies on the effect of curing conditions on the curing rate and mechanical properties of moisture-cured poly(urethane-urea) elastomers containing oligocarbonate segments. *Polimery Journal*. 2011;56(7-8):564-570.

49. Bolasodun B, Nesbitt A, Wilkinson A, Day R. Effect of Curing Method On Physical And Mechanical Properties Of Araldite DLS 772 / 4 4 DDS Epoxy System. *International Journal of Scientific & Technology Research*. 2013;2(2):12-18.

50. Hakimian E, Sulong AB. Analysis of warpage and shrinkage properties of injection-molded micro gears polymer composites using numerical simulations assisted by the Taguchi method. *Materials & Design*. 2012;42:62-71.

51. Quiroga A, Marzocchi V, Rintoul I. Influence of wood treatments on mechanical properties of wood-cement composites and of Populus Euroamericana wood fibers. *Composites Part B: Engineering*. 2016;84:25-32.

52. Hoffman JIE. *Biostatistics for Medical and Biomedical Practitioners*. Oxford: Academic Press; 2015.